Ratios of helicity amplitudes for hard exclusive ρ^0 electroproduction on transversely polarized protons

Charlotte Van Hulse[*]

University of the Basque Country, UPV/EHU
E-mail: cvhulse@mail.desy.de

The HERMES experiment collected a wealth of deep-inelastic scattering data using the 27.6 GeV polarized lepton beam at HERA and various pure gas targets, both unpolarized and polarized. This allowed for a series of diverse measurements. Among them are measurements of hard exclusive meson production, which provide information on generalized parton distributions (GPDs), in a complementary way to, e.g., deeply virtual Compton scattering. Access to these GPDs is possible through the measurement of helicity-amplitude ratios. Helicity-amplitude ratios from exclusive ρ^0 production on transversely polarized hydrogen are presented and discussed as well as compared to the theoretical 'GK' model.

XXV International Workshop on Deep-Inelastic Scattering and Related Subjects
3-7 April 2017
University of Birmingham, UK

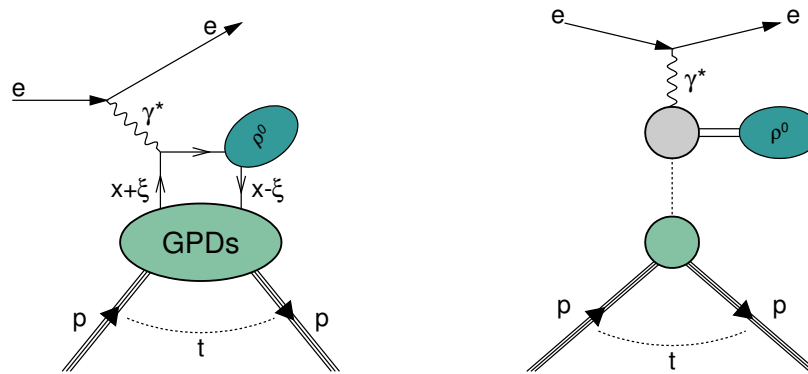
[*]Speaker.

Figure 1: Depiction of the process hard exclusive ρ^0 production.

1. Introduction

Exclusive reactions in deep-inelastic scattering provide access to generalized parton distributions (GPDs). These distributions, being probability amplitudes, do not have a probabilistic interpretation. However, their Fourier transform in a specific kinematic regime, i.e., in absence of longitudinal-momentum transfer, do represent the probability of finding a parton in the nucleon as a function of its transverse position in the nucleon and of its longitudinal-momentum fraction with respect to the longitudinal momentum of the nucleon. The longitudinal direction is here defined as the direction of movement of the fast moving nucleon or, equivalently, as the direction of the probe used to study the nucleon.

There are eight leading-twist GPDs. Four of them involve parton-helicity conservation, while the other four are chiral-odd. A further differentiation of the GPDs relies on the flip or non-flip of the nucleon spin and on the consideration or disregard of the polarization state of the partons. Two GPDs, i.e., GPDs E and H enter the Ji sum rule. This relates the two aforementioned GPDs to the parton total angular momentum [1].

Deeply virtual Compton scattering provides the theoretically cleanest access to GPDs. In particular, it is sensitive to chiral-even GPDs. Hard exclusive electroproduction of mesons offers a complementary channel to probe GPDs. It probes various types of GPDs with different sensitivity and in different flavour combinations. Depending on the produced meson, chiral-odd GPDs can also be accessed. The additional complication of exclusive meson production with respect to deeply virtual Compton scattering is the determination of the meson distribution amplitude, a non-perturbative object, which cannot be determined from first principles.

In the present proceedings, the exclusive electroproduction of ρ^0 mesons from a transversely polarized hydrogen target is discussed. The process is depicted in figure 1, left, under the assumption of one-photon exchange. Here, a virtual photon is absorbed by a quark from the nucleon. Following this, a ρ^0 meson is produced and a quark is absorbed by the nucleon, which stays intact yet with a different momentum. The square of the four-momentum transfer to the nucleon is represented by t. In the case that the nucleon is unpolarized, the GPDs $H, \tilde{H}$ and $\bar{E}_T = 2\tilde{H}_T + E_T$ are probed, while the usage of a transversely polarized nucleon target allows to access GPDs $E, \tilde{E}$, and H_T. Here, the presence (absence) of subscript T indicates chiral-oddness (chiral-evenness). The

chiral-even GPDs indicated with (without) a tilde refer to polarized (unpolarized) quarks.

Alternatively, in the light of Regge phenomenology, one can interpret exclusive electroproduction of ρ^0 mesons as depicted in figure 1, right. Here, the virtual photon splits into a quark-antiquark pair, and this pair interacts with the nucleon through the exchange of a reggeon. The exchanged reggeon can be of natural parity, i.e., with parity $P = (-1)^J$, in which case it corresponds to a pomeron or a $\rho, f_2, \ldots$, or of unnatural parity, i.e., with $P = (-1)^{J+1}$, in which case it corresponds to a $\pi, a_1, b_1 \ldots$. The symbol J represents the reggeon's total angular momentum. In the case of natural-parity exchange (NPE), one is sensitive to the GPDs H, E, and $\bar{E}_T$, while in the case of unnatural-parity exchange (UPE), the probed GPDs are $\tilde{H}$ and $\tilde{E}$. The GPD H_T has no definite parity.

As clarified below, GPDs enter the expression of helicity amplitudes $F_{\lambda_V \lambda_N' \lambda_\gamma \lambda_N}$. These amplitudes describe the process

$$\gamma^*(\lambda_\gamma) + N(\lambda_N) \rightarrow V(\lambda_V) + N(\lambda_N'), \tag{1.1}$$

where the particles' helicity is indicated in parenthesis. In particular, the amplitudes describe the transition of the helicity of the virtual photon to that of the ρ^0 meson. The amplitudes can be decomposed into a natural-parity amplitude, $T_{\lambda_V \lambda_N' \lambda_\gamma \lambda_N}$, and an unnatural parity amplitude, $U_{\lambda_V \lambda_N' \lambda_\gamma \lambda_N}$:

$$F_{\lambda_V \lambda_N' \lambda_\gamma \lambda_N} = T_{\lambda_V \lambda_N' \lambda_\gamma \lambda_N} + U_{\lambda_V \lambda_N' \lambda_\gamma \lambda_N}, \tag{1.2}$$

where each amplitude component is sensitive to specific GPDs.

The observables accessed in the present analysis are the ratios of natural and unnatural-parity amplitudes to the natural-parity amplitude $T_{0\frac{1}{2}0\frac{1}{2}}$, which is the dominant amplitude. The ratios are denoted respectively $t^{(n)}_{\lambda_V \lambda_\gamma}$ and $u^{(n)}_{\lambda_V \lambda_\gamma}$. Here, a short-hand notation is used, based on symmetry relations with respect to the nucleon helicity the amplitudes obey. The superscript $n = 1$ corresponds to nucleon-helicity non-flip, while $n = 2$ corresponds to nucleon-helicity flip.

Another observable that experimentally can be accessed are spin density matrix elements (SDMEs) [2–4]. They can be rewritten in terms of helicity-amplitude ratios. Various SDMEs were extracted previously, among others for ρ^0 mesons, by the HERMES experiment [5].

2. Analysis

The analysed data were collected by the HERMES experiment, at DESY (Hamburg, Germany). Here, longitudinally polarized 27.6 GeV electrons and positrons were scattered off a transversely polarized hydrogen gas target. The forwardly produced particles were detected by the HERMES spectrometer, with the ρ^0 meson reconstructed from its decay pions. The recoil proton stayed undetected. Instead, it is reconstructed through its missing mass. In total, 8741 events identified as originating from exclusive ρ^0 electroproduction are selected. The invariant mass W is required to lie in the interval between 3.0 GeV and 6.3 GeV, and the photon virtuality, Q^2, between 1.0 GeV^2 and 7.0 GeV^2. The variable $-t'$, with $t' = t - t_0$, where $-t_0$ represents the minimal value of $-t$ for given values of Q^2 and W, is restricted to be smaller than 4 GeV^2.

The helicity-amplitude ratios are extracted from data through a fit to the angular distribution of the ρ^0-meson decay pions. Their distribution is characterised by four angles [6]. In total, 25 parameters are fit, taking into account the kinematic dependence of the helicity-amplitude ratios on t and Q^2 by binning the sample in 4×3 cells in $(Q^2, -t')$.
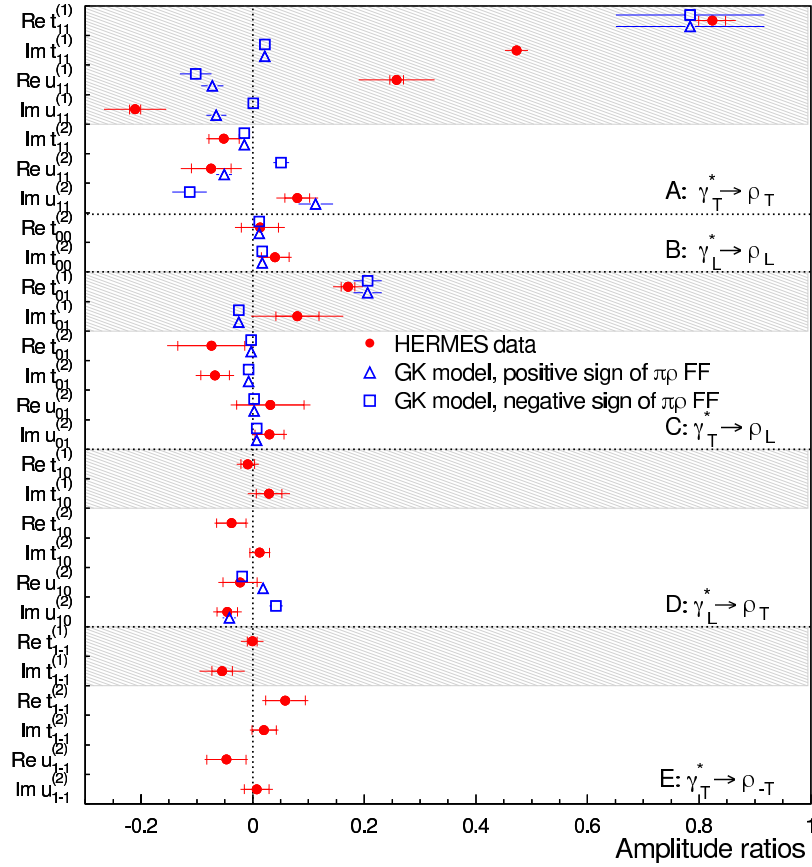
Figure 2: Ratios of ρ^0-meson helicity amplitudes. The inner error bars represent the statistical uncertainty; the outer error bars represent the total uncertainty, obtained by adding statistical and systematic uncertainties in quadrature. For $\Im t_{11}^{(1)}$ only the total uncertainty is shown. An additional scale uncertainty of 2% is present, but not shown, for the ratios $\Im t_{\lambda_V \lambda_\gamma}^{(1)}$, $\Re t_{\lambda_V \lambda_\gamma}^{(2)}$, and $\Re u_{\lambda_V \lambda_\gamma}^{(2)}$ because of the uncertainty on the beam polarization, while an additional uncertainty of 8% is present, but not shown, for $t_{\lambda_V \lambda_\gamma}^{(2)}$ and $u_{\lambda_V \lambda_\gamma}^{(2)}$ because of the uncertainty on the target polarization.

3. Results

The obtained helicity-amplitude ratios are presented in figure 2 by the filled, red circles. They correspond to an average $\langle W \rangle = 4.73$ GeV, $\langle Q^2 \rangle = 1.93$ GeV^2, and $\langle -t \rangle = 0.132$ GeV^2. Note that the value of $\Im t_{11}^{(1)}$ is fixed during the fit and put equal to the result obtained in Ref. [7]. Also the value of the phase of $u_{11}^{(1)}$ is kept fixed and set equal to the result obtained in Ref. [8]. The results represented in front of a shaded background were already obtained previously [7], while those in front of a white background are obtained for the first time (see Ref. [6]). The helicity-amplitude ratios are divided into five clases, depending of the helicity transition of the virtual photon to the ρ^0 meson. Class A (B) corresponds to the transition of a transversely (longitudinally) polarized photon to a transversely (longitudinally) polarized ρ^0 meson. Class C (D) corresponds to the transition of a transversely (longitudinally) polarized photon to a longitudinally (transversely) polarized ρ^0 meson, and class E to a transverse-to-transverse transition but with double helicity flip.

3

From figure 2, it can be seen that the dominant amplitude ratio is the nucleon-helicity-non-flip ratio of natural parity $t_{11}^{(1)}$. It differs from zero by more than 5σ of the total uncertainty. Also $\Re t_{01}^{(1)}$, the real part of the nucleon-helicity-non-flip amplitude ratio of natural parity describing the transition of a transversely polarized photon to a longitudinally polarized ρ^0 meson differs from zero by more than 5σ. The unnatural-parity amplitude ratio without nucleon-helicity flip $u_{11}^{(1)}$ is different from zero, by 4σ. As explained previously, this allows to access polarized GPDs. The nucleon-helicity-flip ratios $\Im t_{01}^{(2)}$, $\Im u_{11}^{(2)}$, and $\Im u_{10}^{(2)}$ are different from zero by 2σ only, while the other nucleon-helicity-flip ratios are equal to zero within roughly 1σ.

4. Comparison with model calculations

In figure 2, also the results of the Goloskokov-Kroll (GK) model calculations are presented [9]. Within the handbag approach, the helicity amplitudes can be written as convolutions of GPDs with appropriate convolution amplitudes. The helicity amplitudes describing helicity conservation from the virtual photon to the ρ^0 meson have following structure:

$$
\begin{aligned}
F_{\lambda_V \frac{1}{2} \lambda_{\gamma=V} \frac{1}{2}} &\propto \sum_{a=q,g} \mathscr{I}\left[A \times \left(H^a, \frac{\xi^2}{1-\xi^2} E^a\right) + A' \times \left(\tilde{H}^a, \frac{\xi^2}{1-\xi^2}\tilde{E}^a\right)\right], \\
F_{\lambda_V -\frac{1}{2} \lambda_{\gamma=V} \frac{1}{2}} &\propto \sum_{a=q,g} \mathscr{I}\left[A \times E^a + A' \times \xi \tilde{E}^a\right],
\end{aligned}
\tag{4.1}
$$

where ξ is a measure for the longitudinal-momentum transfer in the process, and $\mathscr{I}$ indicates the convolution integral of the amplitudes $A^{(')}$ and the respective GPDs. The first equation corresponds to nucleon-helicity non-flip, while the second one to nucleon-helicity flip. Analogous expressions exist for the amplitudes describing a change in helicity from the virtual photon to the ρ^0 meson. Factorization is only proven for the transition of a longitudinally polarized virtual photon to a longitudinally polarized meson. It is assumed in the GK model for the transition of a transversely or longitudinally polarized virtual photon to a transversely polarized meson, while the other transitions are neglected. In order to make the former assumption possible, infrared singularities are regularised by the modified perturbative approach, assuming the partons to be collinear when emitted and absorbed by the nucleon, but to have transverse momentum in the subprocesses describing the interaction with the virtual photon up to the formation of the vector meson.

In the GK model, GPD $\tilde{E}$ is neglected, since it underestimates the pion pole. Instead the pion pole, which goes as $1/(t - m_\pi^2)$, with m_π the pion mass, is treated as the exchange of a neutral pion. This exchanged particle is represented in figure 1, right, by the finely dashed line between the upper, grey circle and the lower, green circle. The virtual photon–pion–ρ^0 meson coupling can be approximated at small $-t$ by the pion–ρ^0 meson transition form factor. The latter is evaluated by weighting the ω–transition form factor according to the respective meson quark content. The magnitude of the ω–transition form factor itself is extracted from HERMES ω-SDME measurements [10]. These are, however, not sensitive to the sign of the form factor. The presented model calculations are thus shown for positive and negative sign of the form factor.

As can be seen from figure 2, there is good agreement between the model and the experimental measurements for $\Re t_{11}^{(1)}$, while for $\Im t_{11}^{(1)}$ the discrepancy between both is large. The amplitude ratio is mostly sensitive to GPD H. The disagreement between model and experimental data for the

imaginary part is partly due to a known underestimate of the relative phase between the amplitudes describing the transverse–transverse and longitudinal–longitudinal polarization transitions between the virtual photon and ρ^0 meson. The helicity-amplitude ratio $u_{11}^{(1)}$, which is mostly determined by GPD $\tilde{H}$ and the pion pole, is not well described by the GK model. The underestimate of the model can be traced back to the neglect of the contribution from GPD $\tilde{E}$ or to an underestimate of the ρ^0 meson–pion transition form factor.

For the nucleon-helicity-flip amplitude ratio $\Im t_{11}^{(2)}$, which receives contributions from GPD E, the model describes the experimental data well. For $\Re u_{11}^{(2)}$ and $\Im u_{11}^{(2)}$, which in the model receives only contributions from the pion pole, good agreement between the model and experimental results is observed in the case of a positive sign of the form factor. Also for $t_{00}^{(2)}$ and $t_{01}^{(1)}$, mainly sensitive to GPDs E and $\bar{E}_T$, respectively, good agreement is observed.

The helicity-amplitude ratios $t_{01}^{(2)}$ and $u_{01}^{(2)}$ receive contributions from GPD H_T. Since this GPD has no specific parity, $u_{01}^{(2)}$ is set equal to $-t_{01}^{(2)}$ in the GK model. The ratios do not receive contribution from the pion pole, thus they cannot decide about the sign of the form factor and the predictions for both signs of the form factor are equal. Apart from a small overestimate of $\Im t_{01}^{(2)}$, the model describes the data well.

The helicity-amplitude ratio $u_{10}^{(2)}$, receiving contribution only from the pion pole, is again able to discriminate the sign of the form factor, and also here a positive sign is favored.

The other helicity-amplitude ratios are set equal to zero in the GK model, which is in agreement with the experimental observation.

As stated, from the obtained helicity-amplitude ratios, SDME values can be obtained. These can be compared to previous direct HERMES measurements of SDMEs [5, 11]. The comparison is not shown here, but it can be found in Ref. [6]. Good agreement is observed between the directly and indirectly extracted SDMEs. However, since both methods of obtaining SDMEs probe a different parameter space, the methods are not necessarily expected to coincide.

References

[1] X. Ji, Phys. Rev. Lett. **78** (1997) 610.

[2] K. Schilling and G. Wolf, Nucl. Phys. B **61** (1973) 381.

[3] H. Fraas, Ann. Phys. **87** (1974) 417.

[4] M. Diehl, JHEP **0709** (2007) 064.

[5] A. Airapetian et al., Eur. Phys. J. C **62** (2009) 659.

[6] A. Airapetian et al., Eur. Phys. J. C **77** (2017) 378.

[7] A. Airapetian et al., Eur. Phys. J. C **71** (2011) 1609.

[8] A. Airapetian et al., Eur. Phys. J. C **29** (2003) 171.

[9] S. Goloskokov and P. Kroll, Eur. Phys. J C **50** (2007) 829; Eur. Phys. J C **53** (2008) 367; Eur. Phys. J A **50** (2014) 146.

[10] A. Airapetian et al., Eur. Phys. J. C **74** (2014) 3110.

[11] A. Airapetian et al, Phys. Lett. B **679** (2009) 100.